The small-x gluon from forward charm production: implications for a 100 TeV proton collider

Rhorry Gauld

ETH Zurich, Institut fur theoretische Physik, Wolfgang-Paulistr. 27, 8093, Zurich, Switzerland.
E-mail: rgauld@phys.ethz.ch

Juan Rojo[*]

Department of Physics and Astronomy, VU University, De Boelelaan 1081, 1081 HV Amsterdam,
and Nikhef Theory Group, Science Park 105, 1098 XG Amsterdam, The Netherlands.
E-mail: j.rojo@vu.nl

Emma Slade

Rudolf Peierls Centre for Theoretical Physics, 1 Keble Road,
University of Oxford, OX1 3NP Oxford, United Kingdom.
E-mail: emma.slade@physics.ox.ac.uk

We review the constraints on the small-x gluon PDF that can be derived by exploiting the forward D meson production data from the LHCb experiment at $\sqrt{s} = 5, 7$ and 13 TeV. We then discuss the phenomenological implications of the resulting improved small-x gluon for ultra-high energy astrophysics, in particular neutrino telescopes, as well as for the proposed Future Circular Collider (FCC) with $\sqrt{s} = 100$ TeV. We illustrate how at the FCC even electroweak scale cross-sections can become sensitive to the small-x region of the quark and gluon PDFs, and then demonstrate how the addition of the LHCb heavy meson production measurements leads to a reduction of PDF uncertainties for various benchmark cross-sections.

---

[*]Speaker.

The small-x gluon from LHCb charm data   The small-x gluon is one of the worse known parton distributions functions (PDFs) of the proton due to the lack of direct experimental information [1, 2]. In global PDF analyses, the small-x region is constrained only by the inclusive and charm HERA structure function data, whose coverage is limited to $x \gtrsim 3 \cdot 10^{-5}$ for $Q^2 \gtrsim 2\,\mathrm{GeV}^2$. Recently, it has been demonstrated [3, 4, 5] that it is possible to constrain this small-x region of $g(x, Q)$ by means of inclusive D and B meson forward production measurements from the LHCb experiment. This sensitivity arises because heavy meson production is driven at the LHC by the gg luminosity, and the unique forward kinematic coverage of LHCb allows to cover the very small-x region. A recent combined analysis [6] of the LHCb measurements of D meson production at $\sqrt{s} = 5, 7$ and 13 TeV showed that it is possible to constrain the gluon PDF reasonably well down to $x \simeq 10^{-6}$, well below the reach of the HERA data.

The differential cross-sections for D meson production are only known at NLO and are affected by rather large theory uncertainties, in particular from scale variations. Therefore, the inclusion of the LHCb D measurements in the global PDF fit requires to introduce normalized cross-sections,

$$N_X^{ij} = \frac{\mathrm{d}^2\sigma(\mathrm{X\ TeV})}{\mathrm{d}y_i^D \mathrm{d}(p_T^D)_j} \Bigg/ \frac{\mathrm{d}^2\sigma(\mathrm{X\ TeV})}{\mathrm{d}y_{\mathrm{ref}}^D \mathrm{d}(p_T^D)_j}, \qquad R_{13/X}^{ij} = \frac{\mathrm{d}^2\sigma(\mathrm{13\ TeV})}{\mathrm{d}y_i^D \mathrm{d}(p_T^D)_j} \Bigg/ \frac{\mathrm{d}^2\sigma(\mathrm{X\ TeV})}{\mathrm{d}y_i^D \mathrm{d}(p_T^D)_j}, \qquad (1)$$

where X represents a center-of-mass energy and y_{ref}^D stands for a fixed reference rapidity bin. In the case of N_X^{ij}, a judicious choice of y_{ref}^D ensures that most theoretical uncertainties are reduced without losing sensitivity to the small-x gluon PDF.

In Fig. 1 we show the small-x gluon from NNPDF3.0 [7] compared with the the results when various combinations of LHCb D meson production data are included in the fit [6], in particular the $N^7 + R^{13/5}$ and the $N^5 + N^7 + N^{13}$ combinations that exhibit similar constraining power. We observe how at small-x the gluon PDF uncertainties can be reduced by up to an order of magnitude as compared to the baseline NNPDF3.0 results. In the same figure we also show the impact of the variations of the input theoretical settings in the $N^5 + N^7 + N^{13}$ NNPDF3.0+LHCb fit, illustrating than in all cases the resulting shifts in the small-x gluon are subdominant or of similar size as the resulting PDF uncertainties, and thus demonstrating the robustness of the analysis.

Implications for high-energy neutrino telescopes   In order to illustrate the implications of the NNPDF3.0+LHCb sets for ultra high energy (UHE) astroparticle physics, in Fig. 2 we show the prompt neutrino flux from Ref. [8] computed in using the NNPDF3.0+LHCb results of Ref. [8] (GRRST) together with the corresponding theory uncertainty band. This prompt flux arises from the decays of D and B mesons produced in cosmic ray collisions in the atmosphere, and is the dominant background for astrophysical UHE neutrinos. We also show the results of the upper bounds from a recent IceCube data analysis. The IceCube bounds are are slightly below the GRRST prediction, suggesting that a first direct detection of the prompt neutrino flux could be within reach.

In Fig. 2 we also show the charged-current (CC) UHE neutrino-nucleus cross-section computed with the NNPDF3.0+LHCb sets. We find that as a consequence of the reduction of the small-x gluon PDF uncertainties, now few-percent theory errors can be achieved up to the most extreme
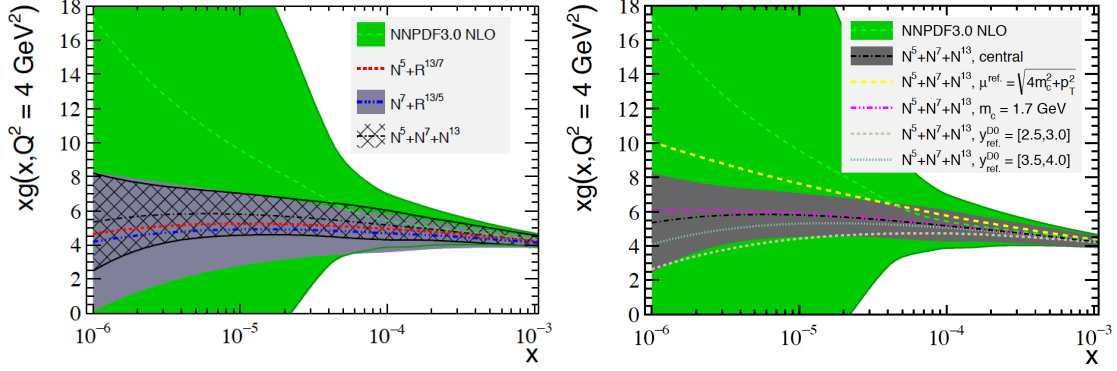
Figure 1: Left plot: the small-x gluon PDF in NNPDF3.0 compared with the results when various combinations of LHCb D meson production data are included in the fit. Right plot: the impact of variations of the input theoretical settings in the $N^5 + N^7 + N^{13}$ NNPDF3.0+LHCb fit.
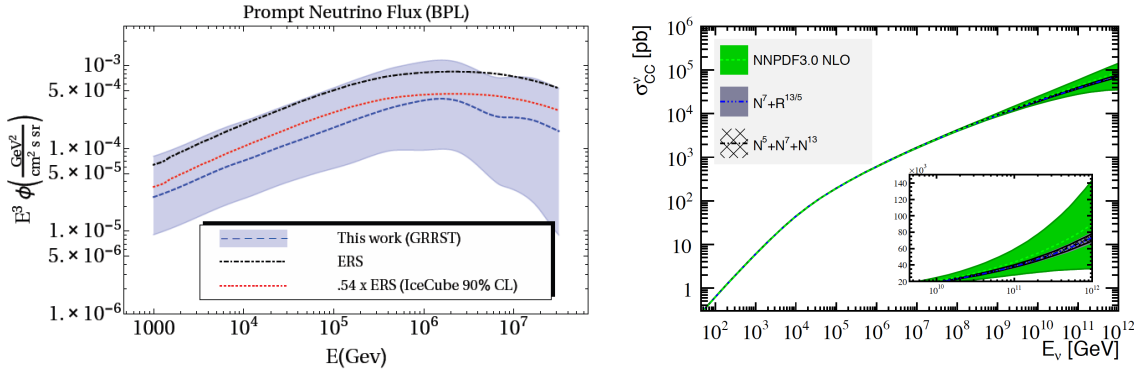

Figure 2: Left plot: the GRRST prompt neutrino flux computed using the N^7 NNPDF3.0+LHCb set with the corresponding theory uncertainty band. We also show the results of a recent upper bound from the IceCube data analysis. Right plot: the charged current UHE neutrino-nucleus cross-section computed with the NNPDF3.0+LHCb sets, compared with the NNPDF3.0 baseline.

neutrino energies, $E_\nu = 10^{12}$ GeV. Having a robust QCD baseline for UHE neutrino-nucleus cross-sections paves the way for novel studies, both in the SM and beyond it, based on upcoming data from neutrino telescopes at these extreme energies. One example would be testing for departures of the linear DGLAP framework by searching for non-linear effects small-x (BFKL) resummation.

Benchmark cross-sections at 100 TeV   At the proposed Future Circular Collider (FCC), operating with a centre of mass energy of $\sqrt{s} = 100$ TeV, many processes will be sensitive to the PDFs down to the very low-x region, $x \lesssim 10^{-5}$, even relatively high-scale processes such as inclusive W or Z production [9, 10]. The accurate determination of the PDFs in this regime is therefore an important ingredient of the FCC physics program. Here we explore the impact that the improved small-x PDFs constrained by the LHCb D meson data, derived in [6], have on a number of important cross-sections for proton-proton collisions at $\sqrt{s} = 100$ TeV.

First of all, we have computed fiducial cross sections for W and Z production using MCFM [11].
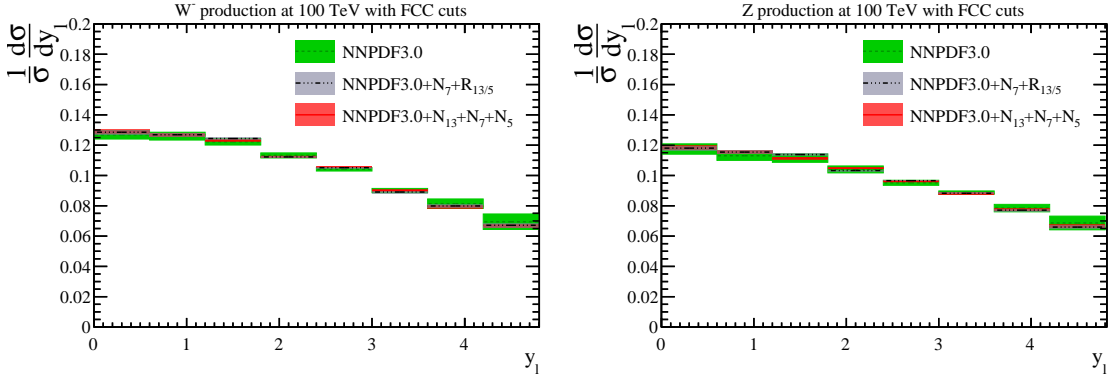
Figure 3: Normalised charged lepton rapidity distributions from W^- (left) and Z (right) boson production at $\sqrt{s}$ = 100 TeV. We show the predictions from NNPDF3.0 and for the two NNPDF3.0+LHCb sets, together with the corresponding PDF uncertainties.

We have produced NLO results for the baseline NNPDF3.0 and for two of the NNPDF3.0+LHCb sets, namely those based on the $N_7+R_{13/5}$ and $N_5+N_7+N_{13}$ combinations. We have considered three different possibilities for the acceptance cuts on the kinematics of the final-state leptons: i) no cuts, ii) "LHC cuts" of $p_T^l \geq 20$ GeV and $|y_l| \leq 2.5$ and iii) "FCC cuts" cuts of $p_T^l \geq 20$ GeV and $|y_l| \leq 5$. The latter cuts are motivated by the expectation that the FCC should have improved coverage of the forward region as compared to the LHC. For Z production, the dilepton invariant mass is restricted to the region $66 \geq m_{ll} \geq 116$ GeV.

In Fig. 3 we show the normalised rapidity distributions of the charged leptons from W^- and Z decays corresponding to the "FCC cuts" scenario, namely where the inclusive cross-section receives contributions from lepton rapidities as large as $|y_l| = 5$. Taking into account the LO kinematics, $x_{1,2} = (M_V/\sqrt{s})e^{\pm y_V}$, where y_V is the gauge boson rapidity, one sees that that PDFs down to $x \simeq 10^{-5}$ are being probed. As expected, we observe a reduction in the corresponding PDF uncertainties specially at high rapidities, which is where the sensitivity to the small-x gluon comes from, once the NNPDF3.0+LHCb sets are used as compared to the baseline NNPDF3.0 results.

This reduction of the PDF uncertainties at large lepton rapidities has direct consequences for the inclusive W and Z cross-sections integrated over rapidity. In Table 1 we list the cross sections times branching ratios $\sigma(V)\mathrm{BR}(V \to l_1 l_2)$ for weak gauge boson production at 14 TeV and 100 TeV for different sets of kinematic cuts. We indicate both the central value (in nb) and the percentage PDF uncertainty for the NNPDF3.0 and NNPDF3.0+LHCb NLO sets, the latter based on the $N^5 + N^7 + N^{13}$ combination. We see that while at 14 TeV the PDF uncertainties are of the same size with and without cuts, at 100 TeV this is not the case: without cuts, the inclusive W, Z cross-sections exhibit PDF uncertainties as large as 7%, and even with the "FCC cuts" they can be up to a factor 2 larger than those corresponding to the "LHC cuts", reflecting the sensitivity to the small-x region. For the NNPDF3.0+LHCb set instead, the PDF uncertainties become essentially independent of the choice of kinematical cuts, highlighting the stabilization of the small-x region.

In addition to inclusive W/Z production, we have calculated other benchmark cross-sections at 100 TeV. To begin with, we have calculated inclusive prompt photon production at NLO with MCFM,

		14 TeV		100 TeV		
		No cuts	LHC cuts	No cuts	LHC cuts	FCC cuts
NNPDF3.0	W^+	11.8 (1.9%)	6.4 (2.0%)	73.5 (7.0%)	27.8 (2.9%)	52.8 (4.9%)
	W^-	8.8 (1.8%)	4.7 (1.4%)	61.9 (5.5%)	26.0 (3.0%)	44.1 (3.6%)
	Z	2.0 (1.7%)	1.5 (1.8%)	14.1 (5.1%)	7.9 (3.2%)	12.5 (4.1%)
NNPDF3.0+LHCb	W^+	12.2 (1.6%)	6.6 (1.7%)	73.4 (3.0%)	29.0 (2.7%)	53.5 (2.8%)
	W^-	9.1 (1.6%)	4.9 (1.7%)	62.3 (2.9%)	27.2 (2.8%)	45.2 (2.8%)
	Z	2.1 (1.6%)	1.5 (1.7%)	14.3 (2.8%)	8.3 (2.9%)	12.8 (2.8%)

Table 1: The cross sections times branching ratios $\sigma(V)\mathrm{BR}(V \to l_1 l_2)$ for weak gauge boson production at 14 TeV and 100 TeV for different sets of kinematic cuts, described in the text. We indicate both the central value (in nb) and the percentage PDF uncertainty for the NNPDF3.0 and NNPDF3.0+LHCb NLO sets, the latter based on the $N^5 + N^7 + N^{13}$ combination.
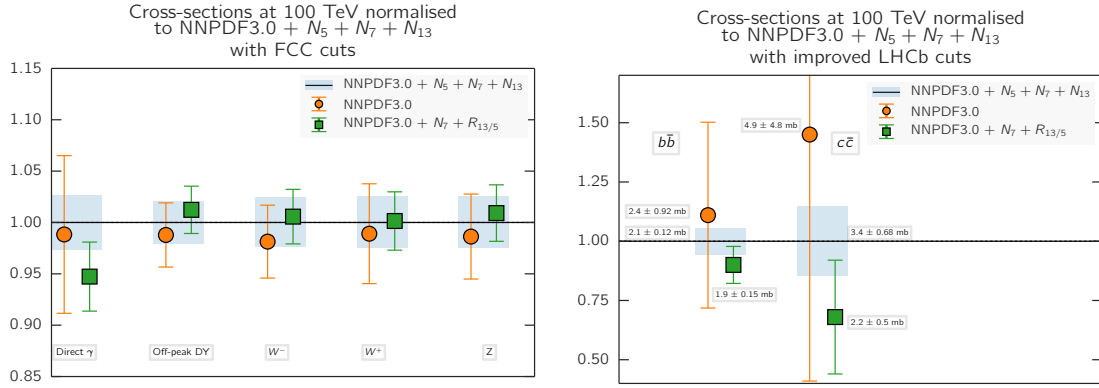

Figure 4: Left plot: inclusive cross sections at NLO with "FCC cuts" (see text) computed with NNPDF3.0 and two of the NNPDF3.0+LHCb sets, normalized to the central value of the $N_5 + N_7 + N_{13}$ fit. The error bands includes only the PDF uncertainties. Right plot: same for charm and bottom pair production, in the fiducial region defined by $2.5 < y_Q < 6.5$.

where the following fiducial cuts have been imposed: $|y_\gamma| < 5$ and $p_T^\gamma > 20$ GeV. Then we have also computed the cross-sections for Drell-Yan γ^*/Z production at low invariant masses, where we require $p_T^l \geq 20$ GeV, $|y_l| \leq 5$, and $20 < m_{ll} < 30$ GeV for the final-state leptons. Both process are characterized by some sensitivity to the small-x region. Moreover, we have also computed heavy quark pair production both for charm and for bottom quarks. In this case we have assumed that the FCC would be equipped with the forward detector, analogous to the LHCb experiment, that can instrument the region $2.5 < y_Q < 6.5$ for the heavy quark rapidity. Heavy quark pair production cross-sections have been computed at NLO using `MadGraph_aMC@NLO` [12] without imposing any cut on the heavy quark p_T^Q.

The overview of the results is presented in Fig. 4, where we compare the various NLO cross-sections, with the "FCC cuts", computed with NNPDF3.0 and the two NNPDF3.0+LHCb sets. In all cases we observe a reduction of the PDF uncertainties as a consequence of the improved small-x gluon PDF. For instance, for direct photon production the PDF uncertainties become smaller by more than a factor of two. Unsurprisingly, the effect is the largest for forward heavy quark produc-

tion, specially in the charm quark case. Using NNPDF3.0, the PDF uncertainties in the fiducial 100 TeV cross-section are around 100%, which are reduced to around 20% once the NNPDF3.0+LHCb sets are used. Fig. 4 thus illustrates how the exploitation of available and future LHC data can improve the prospects of a precision physics program at a future 100 TeV hadron collider. Another example would be the use of top-quark pair differential distributions in the NNLO global fit to constrain the gluon PDF at large x [13], the region relevant for new heavy BSM resonances produced in the gluon-gluon channel.

References

[1] J. Butterworth et al., *PDF4LHC recommendations for LHC Run II*, *J. Phys.* **G43** (2016) 023001, [arXiv:1510.03865].

[2] J. Rojo et al., *The PDF4LHC report on PDFs and LHC data: Results from Run I and preparation for Run II*, *J. Phys.* **G42** (2015) 103103, [arXiv:1507.00556].

[3] R. Gauld, J. Rojo, L. Rottoli, and J. Talbert, *Charm production in the forward region: constraints on the small-x gluon and backgrounds for neutrino astronomy*, *JHEP* **11** (2015) 009, [arXiv:1506.08025].

[4] **PROSA** Collaboration, O. Zenaiev et al., *Impact of heavy-flavour production cross sections measured by the LHCb experiment on parton distribution functions at low x*, *Eur. Phys. J.* **C75** (2015), no. 8 396, [arXiv:1503.04581].

[5] M. Cacciari, M. L. Mangano, and P. Nason, *Gluon PDF constraints from the ratio of forward heavy-quark production at the LHC at $\sqrt{S} = 7$ and 13 TeV*, *Eur. Phys. J.* **C75** (2015), no. 12 610, [arXiv:1507.06197].

[6] R. Gauld and J. Rojo, *Precision determination of the small-x gluon from charm production at LHCb*, *Phys. Rev. Lett.* **118** (2017), no. 7 072001, [arXiv:1610.09373].

[7] **NNPDF** Collaboration, R. D. Ball et al., *Parton distributions for the LHC Run II*, *JHEP* **04** (2015) 040, [arXiv:1410.8849].

[8] R. Gauld, J. Rojo, L. Rottoli, S. Sarkar, and J. Talbert, *The prompt atmospheric neutrino flux in the light of LHCb*, *JHEP* **02** (2016) 130, [arXiv:1511.06346].

[9] M. L. Mangano et al., *Physics at a 100 TeV pp collider: Standard Model processes*, arXiv:1607.01831.

[10] J. Rojo, *Parton Distributions at a 100 TeV Hadron Collider*, *PoS* **DIS2016** (2016) 275, [arXiv:1605.08302].

[11] R. Boughezal, J. M. Campbell, R. K. Ellis, C. Focke, W. Giele, X. Liu, F. Petriello, and C. Williams, *Color singlet production at NNLO in MCFM*, *Eur. Phys. J.* **C77** (2017), no. 1 7, [arXiv:1605.08011].

[12] J. Alwall, R. Frederix, S. Frixione, V. Hirschi, F. Maltoni, et al., *The automated computation of tree-level and next-to-leading order differential cross sections, and their matching to parton shower simulations*, *JHEP* **1407** (2014) 079, [arXiv:1405.0301].

[13] M. Czakon, N. P. Hartland, A. Mitov, E. R. Nocera, and J. Rojo, *Pinning down the large-x gluon with NNLO top-quark pair differential distributions*, *JHEP* **04** (2017) 044, [arXiv:1611.08609].